Decadal-scale morphological adjustment of a lowland tropical river

Elizabeth H. Dingle[a,b]*, Enrico C. Paringit[c], Pamela L.M. Tolentino[d], Richard D. Williams[a], Trevor B. Hoey[a], Brian Barrett[a], Hazel Long[a], Crystal Smiley[a], Eilidh Stott[a]

[a.] School of Geographical and Earth Sciences, University of Glasgow, United Kingdom

[b.] Department of Geography, Faculty of Environment, Simon Fraser University, Canada

[c.] Geodetic Engineering, University of Philippines – Diliman, Philippines

[d.] National Institute of Geological Sciences, University of Philippines – Diliman, Philippines

* Corresponding author. E-mail address: elizabeth_dingle@sfu.ca (Elizabeth H. Dingle)

Abstract

Compared with temperate regions, much less is known about the dynamics of tropical river systems. Tropical rivers are typically characterised by pronounced seasonal changes in precipitation, large sediment loads and high rates of lateral channel migration across often very low-gradient and densely populated floodplains. Understanding the controls on channel migration or change is integral to our ability to fully predict and build resilience against flood risk and wider river-related hazards. Here, we analyse channel and confluence migration over the last ~40 years along a ~85 km reach of the Cagayan River and one of its tributaries, the Pinacanauan de Ilagan (Luzon, Philippines) using optical satellite imagery captured during this period. Combining this with spatial variations in channel pattern, valley width and new bed material grain size data, we demonstrate that sediment transport and deposition are key drivers of the observed tropical channel morphodynamics in this region. The high sediment supply generated in the catchment headwaters (by mass-wasting of hillslopes triggered especially in typhoons) results in high aggradation rates and channel widening on the lower gradient alluvial plain. We suggest that this aggradation enhances local confluence and lateral channel migration rates, which can reach more than 300 m per decade, and that lateral

migration rates of tropical rivers are typically greater than those of temperate rivers. Channel morphodynamics have implications for how to best manage these types of tropical river systems, where hard bank protection structures may result in a complex geomorphic response and flood risk mapping may need to include assessment of sensitivity to varying channel position and topography.

Keywords**:** tropical rivers, channel migration, sediment dynamics, flood risk, Philippines

1. Introduction

Tropical river systems are often characterised by highly seasonally variable water discharges, large sediment loads (e.g., Milliman and Meade, 1983; Gran et al., 2011; Syvitski et al., 2014) and rapid lateral channel migration rates (e.g., meander migration, avulsion, chute cut-off) across low-gradient and, in many instances, densely populated alluvial floodplains (Ashworth and Lewin, 2012; Darby et al., 2013; Constantine et al., 2014; Dixon et al., 2018; Suizu and Nanson, 2018). As channels migrate, they erode large parts of their floodplain which can result in the loss of property, infrastructure and productive farmland. These mobile channels also control patterns of sediment storage and release across the catchment, which influence downstream sediment budgets and pollutant transfer pathways (e.g., mine tailings) (Aalto et al., 2008). Understanding the controls on channel migration or change is integral to our ability to fully predict and build resilience to both flood risk and wider river-related hazards across these dynamic landscapes. Such understanding is paramount in large Asian river systems, where the effects of climate change are predicted to have the greatest impact on future global flood risk (Tolentino et al., 2016; Alfieri et al., 2017) as a result of changing El Niño Southern Oscillation (ENSO) conditions and seasonal rainfall patterns.

Compared with temperate regions, less is known about the behaviour of tropical rivers, defined here as being those located within the tropical climate belt and so experiencing warm

temperatures with little intra-annual variability, and having significant seasonal changes in precipitation (e.g., Syvitski et al., 2014). Many tropical regions are also prone to extreme meteorological events (e.g., typhoons, tropical cyclones), driving short-lived and highly elevated water and sediment discharges. It has been shown that: (i) tropical river channel patterns are not well-represented in global databases; (ii) the controls over sediment transport and channel change may differ from more temperate regions due to differences in hydrology (strong seasonality, typhoon event frequency and magnitude) and catchment properties (soil type, land use and disturbance); and, (iii) channel response to environmental disturbance is significant in the cases where it has been quantified (e.g., Latrubesse et al., 2005; Syvitski et al., 2014; Dewan et al., 2017; Horton et al., 2017). Whether controls on tropical river morphology and dynamics are fundamentally different from those in more temperate settings remains unresolved within the literature (Latrubesse et al., 2005; Scatena and Gupta, 2013; Syvitski et al., 2014; Plink-Björklund, 2015). More recently, changes in tropical forest cover has also been demonstrated to enhance lateral rates of channel mobility through a reduction in bank shear strength and changes in pore water pressure (and therefore bank sediment cohesion) as a result of reduced rainfall interception by forest canopy cover (Horton et al., 2017). Deforestation in the Kinabatangan River (Malaysia) has been suggested as the principal driver of enhanced lateral channel migration rates, by over 20%, in comparison to forested regions over the same 25-year period (Horton et al., 2017). However, the effects of deforestation and land use change on lateral channel migration rates have only been tested in a limited number of tropical systems to date. While enhanced migration rates through changes in land use in tropical environments have been previously documented (e.g., Horton et al., 2017), these trends are not consistent in all tropical environments. The Aguapeí River in Brazil was largely deforested by 1962, yet channel migration rates were found to decrease between 1962-2010 (Suizu and Nanson, 2018). This was attributed to an ENSO-driven increase in peak flow discharge resulting in channel widening and a reduction in channel sinuosity.

This paper presents and analyses new data on channel and confluence migration, channel pattern, width and sediment grain size from a tropical river system. The analysis tests the hypothesis that tropical rivers have higher migration rates than comparable temperate systems (e.g., similar catchment area, gradient, annual mean flow), and that these migration rates may be independent of land use change. We examine a range of factors (e.g., climate and hydrology) that may result in tropical rivers having different morphological characteristics. We first test whether boundary conditions in tropical river systems, which differ from those in temperate rivers, drive high migration rates. The key boundary conditions in this landscape are rates of sediment supply from upstream and the magnitude and frequency of flood hydrographs, dominated by typhoons which generate several geomorphically effective flows each year. We quantify rates of lateral channel migration based on observations over the past ~40 years and then examine confluence migration patterns, channel pattern, width, valley confinement and downstream bed grain size variation and consider the impact of sediment dynamics on modern river morphology. Channel morphology and rates of change are compared with published data to allow evaluation of the hypothesis above. Finally, we explore whether lateral channel and confluence migration represents a significant hazard to communities living along tropical river banks and consider the implications for river and flood risk management.

Analysis was undertaken on the Cagayan River (27,700 km^2) where it passes through Isabela province, in the eastern part of Luzon Island in the Philippines (Fig. 1). The extensive alluvial floodplain of the main Cagayan channel and a number of its tributaries make this an ideal setting to observe large scale patterns of sediment erosion, deposition and channel migration over a period of ~40 years (the period over which satellite imagery is available). The Cagayan River is the largest river system on Luzon and supplies fresh water and nutrient rich sediments to a catchment population of more than 3.45 million (2015 census data). Typically, the Philippines experiences multiple typhoons each year, although not all represent significant hazards. Typhoons of particular note in the last 15 years include Typhoons Haururot (known

internationally as typhoon Imbudo, 2003), Lando (Koppu, 2015) and Lawin (Haima, 2016), which resulted in more than $300 million USD of damage across the Cagayan catchment (mainly to infrastructure and agricultural land), over 100 deaths and the displacement of more than 100,000 people nationwide (Floresca and Paringit, 2017). Typhoon Ompong (Mangkhut) in September 2018 caused significant damage and loss of life after the fieldwork reported in this paper. Despite this risk, populations living on the Cagayan River floodplain have continued to expand by 1-2% annually due to economic opportunities from tilling its fertile soils (Balderama et al., 2017). Deforestation across Luzon Island may have impacted sediment dynamics across parts of the Cagayan catchment. Analysis of maps (1934) and Landsat satellite imagery (captured in 2010) suggest a ~60% reduction in forest cover across the Philippines over this 76-year period (Forest Management Bureau, 2013). Under these conditions, an improved understanding of how sediment dynamics influence channel mobility is paramount in developing effective river management, hazard mitigation and land use strategies.

1.1. Regional geomorphological context

Luzon Island has a diverse tectonic, geologic, and climatic setting which generates spatial differences in the geomorphological characteristics, including topographic relief, channel gradient, drainage density and floodplain confinement of catchments and their river channels. These characteristics result from the nature and rates of processes through which sediment is eroded from the landscape (e.g., Tucker and Slingerland, 1997; Perron et al., 2008; Clubb et al., 2016) and drive variability in channel morphology (e.g., channel planform, lateral migration rate) and patterns of sediment storage and release as sediment is transported through the catchment (Lauer and Parker, 2008). The Cagayan River is the largest catchment on Luzon Island, covering an area of ~27,700 km^2 and is formed of four major tributaries (the Magat, Chico, Ilagan and Pinacanauan rivers), sourced in the surrounding Caraballo, Cordillera and Sierra Madre mountain ranges. The Pinacanauan de Ilagan River, catchment

141 area ~3,000 km^2, drains the south east region of the Cagayan catchment. The Abuan (490
142 km^2) and Bintacan (111 km^2) Rivers form the northeast portion of the Pinacanauan de Ilagan
143 catchment (Fig. 1) and the headwaters of both are in the Sierra Madre mountain range, with
144 a maximum elevation of 1,871 m (Mt. Cresta). The portion of the Pinacanauan de Ilagan
145 catchment which does not include the Bintacan or Abuan catchments shall be referred to as
146 the Ilagan catchment, as shown in Fig. 1a. The western portion of the Northern Sierra Madre
147 mountain range, particularly in the province of Isabela, is characterised by Eocene to
148 Oligocene bedded meta-volcanics, meta-sediments, and basaltic to andesitic flow deposits of
149 the Caraballo Formation. Coarse crystalline diorite intrusions that are possibly from the
150 Dinalungan Diorite Complex are also noted within the region (Mines and Geosciences Bureau,
151 2010). Late Pliocene to Early Pleistocene conglomerates consisting of andesite porphyry
152 clasts of the Ilagan formation are also observed along the Ilagan River.
153
154
155

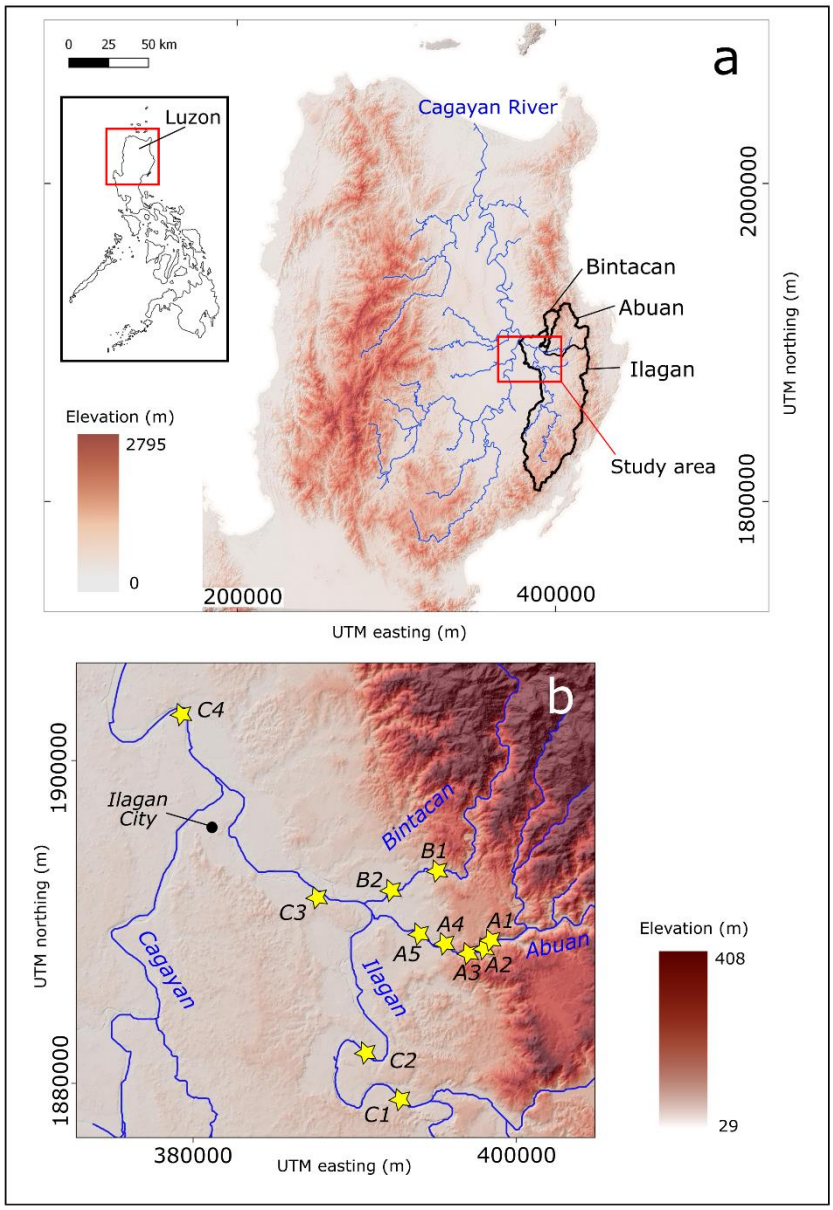

156

157 Fig. 1. a) Location of Luzon Island and the Cagayan basin. The Ilagan, Abuan and Bintacan catchment
158 boundaries are shown in black. The study area is denoted by the red box. b) Study area and surface
159 grain size measurement sites (yellow stars). Coordinates are projected in UTM Zone 51N.

160

161 The Pinacanauan de Ilagan River catchment experiences relatively subdued seasonality
162 (Tolentino et al., 2016), but monthly discharge data shows a drier period between November
163 and April (Fig. 2). Modelled water balances under a range of future climate scenarios across
164 the Philippines have suggested an overall increase in annual water availability, with the
165 proportionally largest increases in peak river runoff predicted for catchments on Luzon Island

(Tolentino et al., 2016). This northern region of Luzon Island experiences several typhoons each year (generally between October-January, Fig. 3), generating significant overbank flooding and damage to local communities (Rojas, 2014). These short-lived (~24 to 48 hour), high magnitude flows (>10,000 m^3/s) (Fig. 3) also generate and transport large quantities of sediment from the Sierra Madre mountains, driving channel bed aggradation and bank erosion further downstream where lower gradient and laterally extensive floodplains have developed.

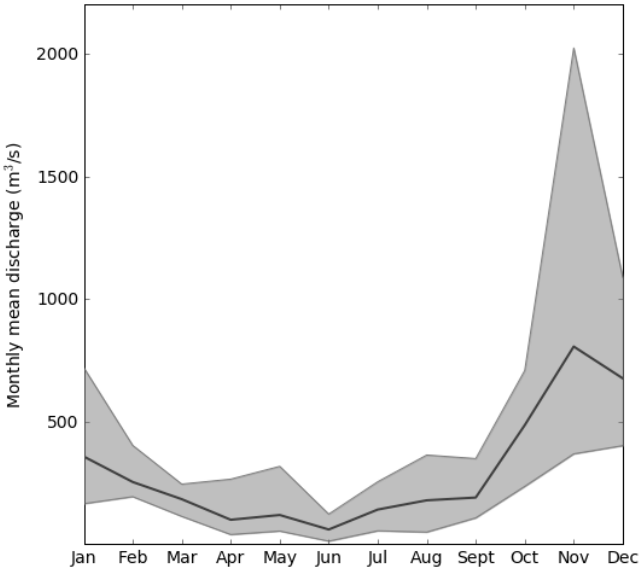

Fig. 2. Mean monthly discharge between 1985 and 2010 for the Pinacanauan de Ilagan River at Ilagan City, where maximum and minimum monthly averages are shown by the grey envelope.

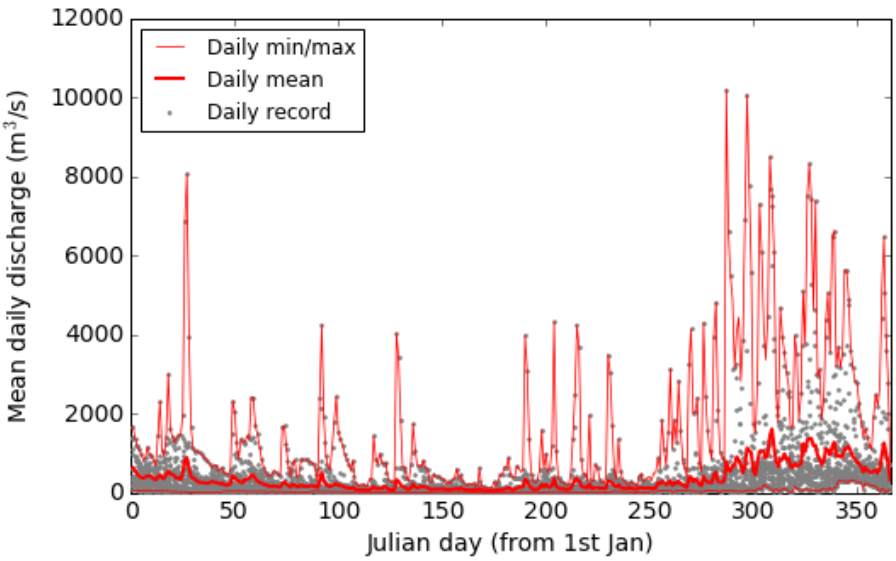

Fig. 3. Measured mean daily discharge (grey dots) at Ilagan, 1985-2010. Daily minima and maxima are shown in thin red lines, whilst the mean value for each calendar day over the entire period is shown by the thicker red line.

Floodwaters generated by Typhoon Lawin (in 2016) in the Bintacan and Abuan catchments mobilised substantial quantities of coarse sediment from the catchment headwaters. These coarse sediments were subsequently deposited in the lower reaches of the Bintacan and Abuan catchments driving lateral bank erosion, loss of floodplain and channel re-organisation. Locally, this resulted in the loss of ~10 properties due to bank erosion along the Bintacan River, as well as damage to transport infrastructure (Fig. 4). Changes in channel bed elevation driven by sediment deposition in the lower reaches of the catchment are also likely to compound flood risk where the gradient of the landscape is very low and tributary confluences are closely spaced. Changes in the base level of either the tributaries or the main river may also influence the backwater length and water depths at channel confluences (Samuels, 1989; Ferguson et al., 2006).

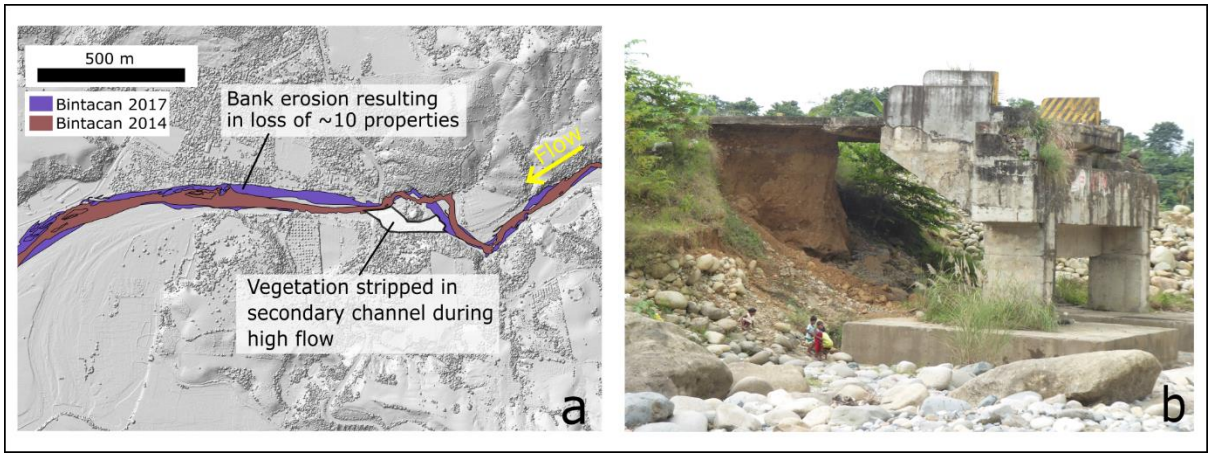

Fig. 4. a) Lateral erosion of the Bintacan channel in response to Typhoon Lawin (2016), resulting in the loss of several properties on the right bank, destruction of the road bridge, and significant reworking and transport of coarse sediment through the reach. The brown shading represents the channel position in 2014 whilst the purple represents the 2017 channel. b) Example of infrastructure damage caused by Typhoon Lawin on the Bintacan channel (17º07'12.83"N, 122º00'41.60"E) where a major road bridge was destroyed and significant coarse sediment deposition occurred.

2. Methods

2.1. Channel and confluence migration

Sediment exchange between the channel and floodplain can form a substantial component of modern river sediment loads. For example, sediment budget estimates derived from optical satellite images and ^{210}Pb geochronology along the Strickland River in Papua New Guinea suggested that floodplain recycling could account for as much as 50% of the total river sediment load (Aalto et al., 2008). Here, we quantify rates of confluence and lateral channel migration using satellite imagery spanning the past ~40 years from Landsat and Sentinel-2 satellite missions (see Table S1 for details).

The positions of major channel confluences across the study area were identified from each scene to examine and quantify patterns of confluence migration, the drivers of which are

broadly similar to those driving lateral channel migration (Dixon et al., 2018). Where systems have high sediment supply, easily erodible floodplains and variable discharges (e.g., monsoon-dominated climates), large river confluences can be highly mobile (Best and Ashworth, 1997; Dixon et al., 2018). Confluences of interest were limited to those with channels wide enough (>60 m) to be clearly identified on older satellite images with lower spatial resolution; these included the Cagayan-Ilagan, Abuan-Ilagan and Bintacan-Ilagan confluences.

Lateral channel migration rates were calculated from manually digitising channel bank positions from imagery captured in 1973, 1990, 2001, 2008 and 2017. This analysis has been restricted to the Ilagan and Cagayan channels within the study area, as lower resolution imagery from earlier Landsat missions was too coarse to distinguish either the smaller Abuan or Bintacan channels. Channel centerlines and lateral migration rates of individual meander bends were then calculated in ArcGIS 10.4 using the Stream Restoration Toolbox (Planform Statistics Tool) described in Aalto et al. (2008).

2.2. Channel pattern

Channel pattern has been strongly correlated with upstream sediment supply (e.g., Schumm, 1985; Miller and Benda, 2000; Church, 2006; Eaton et al., 2010). As sediment supply to a single-thread channel increases, a response in channel pattern is likely to occur (i.e. transition from single-thread to braided) (Mueller and Pitlick, 2014). The more dynamic nature of braided channels allows the system to maintain equilibrium transport conditions under higher sediment supply conditions (Leopold and Wolman, 1957; Smith and Smith, 1984; Eaton et al., 2010; Mueller and Pitlick, 2014), where braided channels are more commonly associated with physiographic settings with steeper channel gradients and higher runoff that yield high stream power compared to single-thread meandering channels (Ashmore, 2013). As such, changes in channel pattern may reflect changes in sediment supply, or channel gradient, within the

Ilagan catchment. Channel sinuosity and braiding intensity were then assessed using GoogleEarth imagery by comparing the down-valley and channel centreline distances between two points, and the total length of all braid channels relative to the length of the channel thalweg between two points (Mosley, 1981), respectively. Points or reaches were spaced where distinct changes in channel morphology could visually be distinguished along continuous reaches (e.g., transitioning from confined to unconfined floodplain conditions), or at channel confluences. In addition to the Pinacanauan de Ilagan River, channel pattern was also assessed further downstream along the full length of the Cagayan River. The confined bedrock portions of the Bintacan and Abuan catchments were not considered.

Transitions from single-thread to braided reaches can also be caused by lateral valley constriction (which initiates bed aggradation) or changes in sediment grain size delivered from tributaries (Mueller and Pitlick, 2014), in addition to changes in channel slope (e.g., Leopold and Wolman, 1957; Van den Berg, 1995; Dade, 2000). For comparison with previous studies, a dimensionless discharge (Q^*) (Parker, 1979; Eaton et al., 2010; Mueller and Pitlick, 2014) is defined as

$$Q^* = \frac{Q_{bf}}{(\sqrt{(s-1)gD_{50}})D_{50}^2} \quad [1]$$

where D_{50} is the median grain size from each sampling location, Q_{bf} is bankfull discharge (m^3/s) and (s-1) is the submerged specific gravity of the sediment. Reach slopes were taken as averages over 10 km, this length being chosen to reduce the effect of artificial noise from the airborne IfSAR (interferometric synthetic aperture radar) DEM (acquired in 2013), as calculation of very low gradients can easily be biased by artificial steps in the topographic data. Bankfull discharge estimates of 2000, 800 and 4000 m^3/s were made for the Abuan, Bintacan and Ilagan channels, respectively, by Rojas (2014) using preliminary hydrological modelling. These bankfull discharge values are conservatively varied by ±50% in our calculations of Q^*

to account for uncertainty in these estimates. Rainfall-runoff modelling predictions by McMillan et al. (2010) suggested that simulations of flood peaks can be under-estimated by almost 50% in these types of models. Dimensionless discharge values were then plotted against channel gradient at each grain size sampling location and compared to previously published data (Mueller and Pitlick, 2014) to examine whether observed channel patterns match predicted patterns based on the published relationships between channel slope, bankfull discharge, sediment grain size and bank strength (Eaton et al., 2010; Mueller and Pitlick, 2014). Using these data, it is possible to examine whether changes in channel planform are related to changes in sediment supply across the Ilagan catchment.

2.3. Channel width

Discharge (Q) is typically related to channel width (w) by a relationship of the form $w \propto Q^b$ (e.g., Leopold and Maddock, 1953; Church, 1992; Wobus et al., 2006) where the exponent b ranges between 0.3-0.6, although few previous studies have specifically focused on tropical river systems. Bankfull width was measured at eight transects spaced 100 m upstream and downstream of 16 tributary junctions across a range of rivers within the Cagayan catchment that were wide enough (>100 m) to have errors of <10% in making measurements from the remote sensing images. Measurements were made from a combination of Sentinel 2 and RapidEye satellite images and excluded mid-channel bars which were densely vegetated and therefore unlikely to be submerged for extensive periods (details in Table S1). Average upstream (w_u), downstream (w_d) and tributary (w_t) widths were calculated from these measurements at each site. Following Ferguson and Hoey (2008), changes in channel width at tributary junctions are predicted from hydraulic geometry relationships as;

$$w_d = w_u\left[1 + (w_t/w_u)^{1/b}\right]^b \quad [2]$$

where b = 0.5 (e.g., Leopold and Maddock, 1953; Richards, 1980; Church, 1992). Solving equation [2] provides predicted downstream channel widths (w_{pd}) using measurements of w_u and w_t at each of the sixteen tributary junctions;

$$w_{pd}^2 = w_u^2 + w_t^2 \quad [3]$$

2.4. Sediment grain size

Surface sediment grain size distributions were collected along the Ilagan, Bintacan and Abuan channels on exposed gravel bar heads at low flow using Wolman counts in January 2018 (Wolman, 1954) on sample sizes of ~300 at each site to ensure precision of the order of ±0.1ψ units for D_{50}, where $2^{\psi} = D$ (Rice and Church 1996; Fig. 1).

3. Results

3.1. Lateral channel and confluence migration

A number of channel confluences within the Ilagan catchment were highly mobile between 1973 and 2017, migrating net distances of more than a kilometre over this ~40-year period. Patterns of confluence node migration for the three most mobile confluences are shown in Fig. 5. Between 1973 and 1990 a partial avulsion also occurred on the Abuan forming a new channel between the Abuan and Bintacan rivers, approximately 2-3 km upstream of their respective confluences with the Ilagan channel.

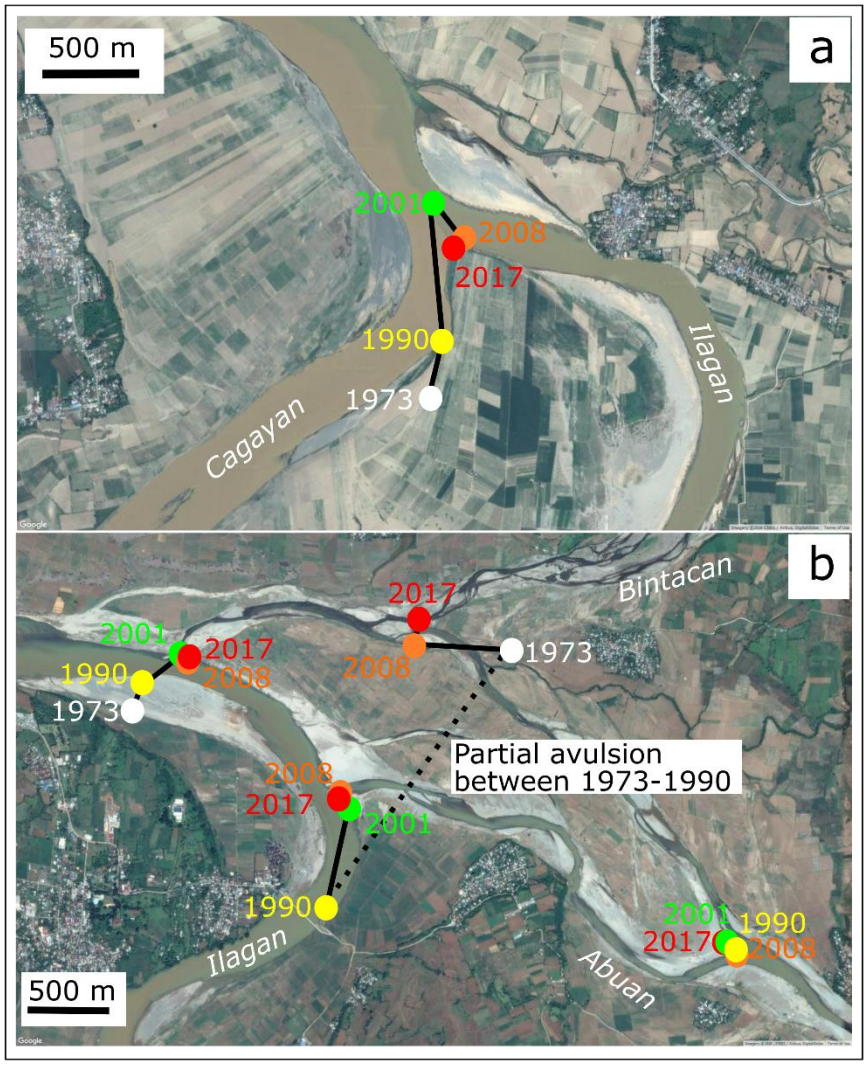

Fig. 5. a) Patterns of confluence node migration between 1973 and 2017 at the Cagayan-Ilagan confluence; and, b) at the Bintacan and Abuan confluences with the Ilagan channel. In 1973, the Abuan channel discharged into the Bintacan channel rather than directly into the Ilagan. A partial avulsion occurred between 1973 and 1990, however, such that the Abuan can now discharge directly into the Ilagan. The base maps for both images are from 2017 in GoogleEarth.

Channel migration rates averaged over four time periods between 1973 and 2017 are shown in Fig. 6a. These rates have been normalised to decadal averages based on the differing time intervals between available images, which spanned from 7 (2001-2008) to 17 (1973-1990) years. In general, the highest decadal migration rates were observed at meander numbers 3, 4, 5, 7 and 9 with the period 1990-2001 showing the highest rates (over 300 m per decade at

meander 7). High rates of lateral meander migration are observed for channels across a range of spatial scales, from highly sinuous smaller tributaries where meander cut-offs are also prevalent (Fig. 6b), to the larger Cagayan River further downstream where meander migration has occurred at kilometre scale between 1973-2017, and older palaeo-channels are preserved considerable distances (~5 km) away from the modern channel (Fig. 6c). Lower meander migration rates at meanders 1, 2, 6 and 8 may relate to local confinement of the channel where the valley bottom is topographically constricted (Fig. 7a), which will inhibit significant lateral migration.

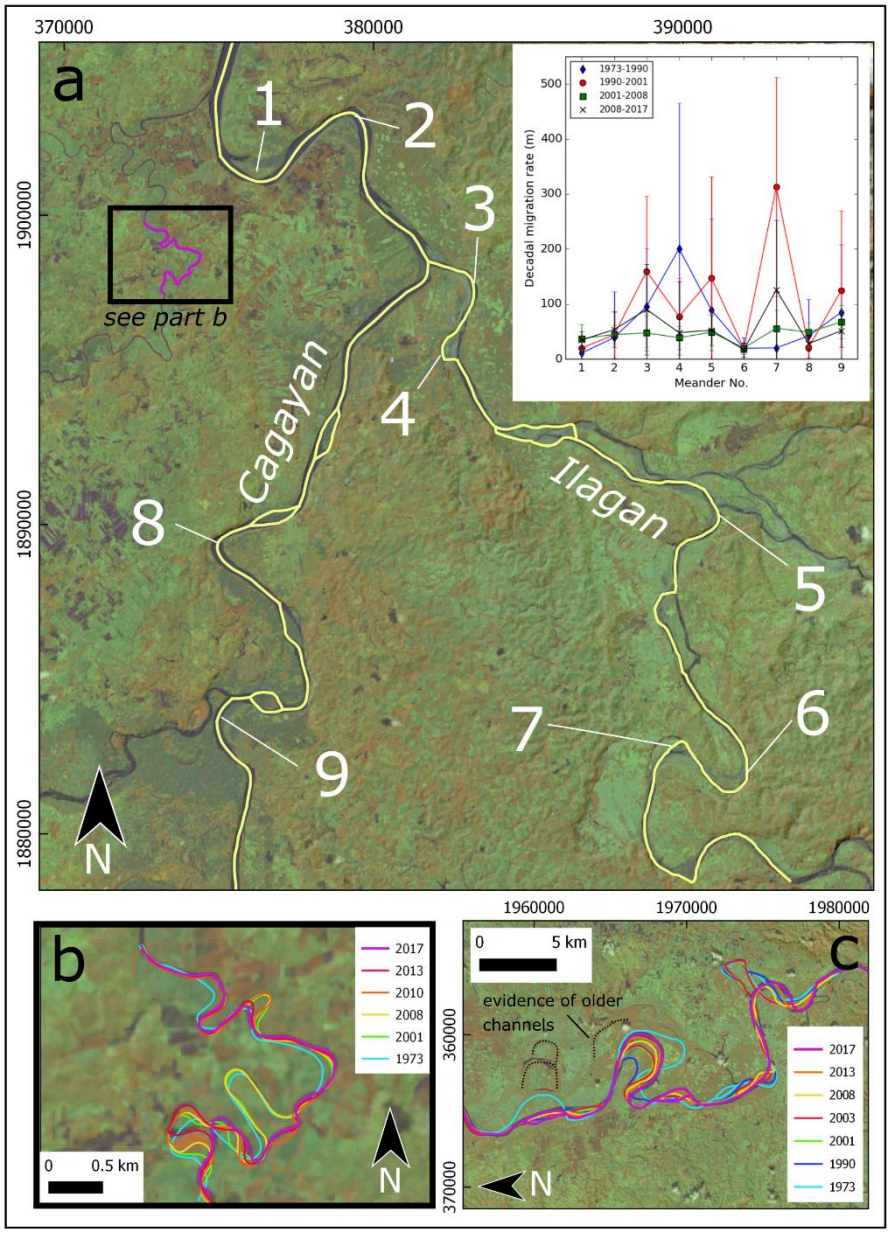

Fig. 6. a) Lateral channel migration rates for individual meanders (numbered 1-9) derived using methods described in Aalto et al. (2008). Rates calculated between images have been normalised to decadal migration rates where the marker represents the average migration rate of the entire meander, and error bars represent +/- 1 standard deviation in rates calculated for each reference point around the individual meander. The base map and yellow centreline represents the 2017 channel position. The extent of this study area is shown by the red box on Fig. 1a. b) Channel positions between 1973 and 2017 for a small tributary of the Cagayan, where the location is shown by a black box in part a. c) Channel positions between 1973 and 2017 along the larger Cagayan system further downstream of Ilagan City. Meander scarps and evidence of kilometre scale channel migration (chute cut-off) prior to 1973 are clearly visible across the Cagayan Valley.

3.2. Channel pattern

Sinuosities calculated from GoogleEarth imagery (captured in June 2017) are generally highest upstream of the Bintacan and Abuan confluences in the Ilagan channel (2.02 and 1.69) (Fig. 7a). Where the Bintacan and Abuan channels exit their confined channels in the Sierra Madre mountains, braiding intensity is also relatively high, as aggradation occurs in response to the lower channel gradient and loss of lateral confinement. Where these two tributaries enter the Ilagan channel, channel sinuosity decreases from 2.02 to 1.29 and braiding intensity increases from 1.24 to 1.85 (Fig. 7a). These changes are consistent with an increase in sediment supply to the Ilagan channel from the Bintacan and Abuan tributaries. In comparison to the Ilagan channel upstream of the Cagayan-Ilagan confluence at Ilagan City, the Cagayan River is generally slightly more sinuous, and is essentially single-thread. Downstream of the Cagayan-Ilagan confluence, channel sinuosity increases along the Cagayan River (Fig. 7b). Braiding intensity was not calculated along the main Cagayan River as the channel is essentially single-thread.

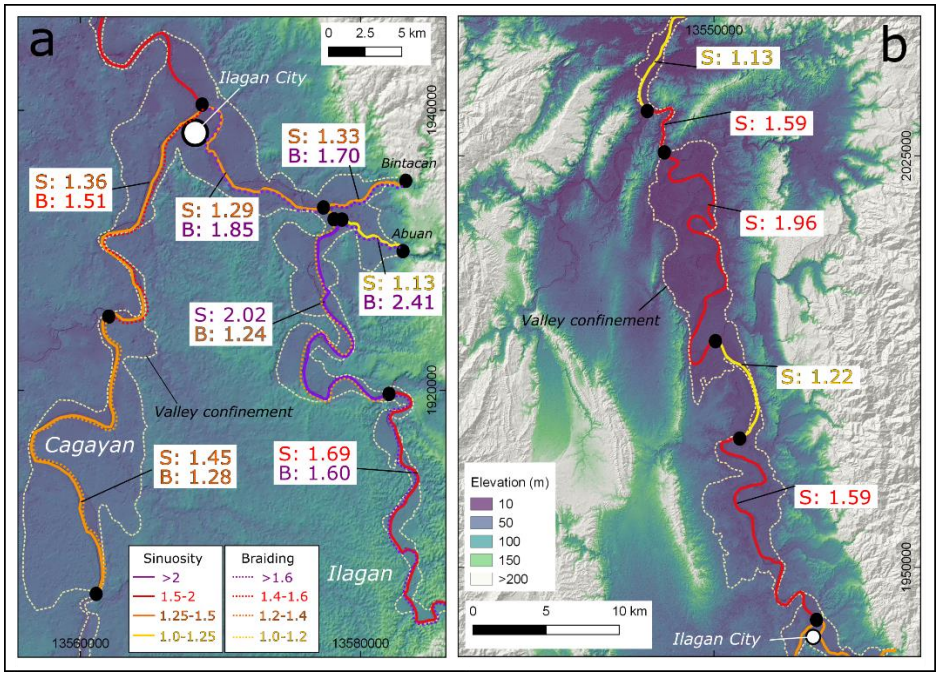

Fig. 7. a) Channel sinuosity (solid line) and braiding intensity (dashed line) on the Ilagan, Bintacan and Abuan channels upstream of Ilagan City. b) Channel sinuosity on the Cagayan between Ilagan City and the Cagayan delta. In both figures, yellow lines represent the lowest sinuosity (and braiding intensity), purple lines represent the highest and orange and red colours represent intermediate values (shown in the key on panel a). The extent of the valley floor or floodplain (valley confinement) is also shown for each panel, and was determined by where either a break or change in valley bottom slope was observed.

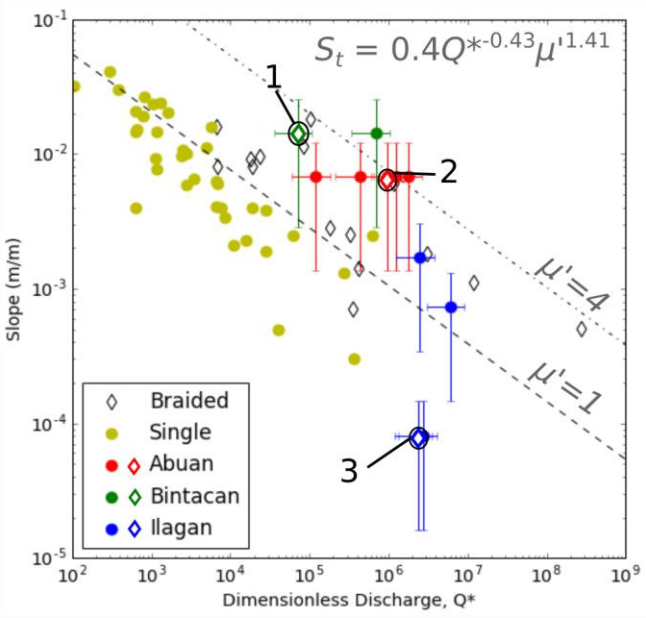

Fig. 8. Dimensionless discharge, Q*, plotted as a function of channel slope, S. Braided and single-thread channel data from a global compilation of rivers presented in Mueller and Pitlick (2014) are shown in black outlined diamonds and filled yellow circles, respectively. New data from this study are shown by coloured solid circles (single-thread) and outlined diamonds (braided). Horizontal error bars represent Q* generated by varying bankfull discharge by ±50%, and vertical error bars represent slope within ±80% of the value calculated from the DEM. Dashed lines represent the relationship between S_t (the threshold slope between braided and single-thread channels) and Q* from Eaton et al. (2010) used to differentiate braided from single-thread channels, using two different dimensionless relative bank strength (μ') values of 4 and 1. Highlighted data points (labelled 1, 2, and 3) relate to samples collected during this study from braided channels, where all other points are from single-thread reaches.

Previous studies have found relationships between dimensionless discharge, channel slope and channel pattern (e.g., Eaton et al., 2010; Mueller and Pitlick, 2014), but the Ilagan, Abuan and Bintacan channels are inconsistent with these result (Fig. 8). Only two of the three braided sites were consistent with previous measurements of braided channels (labelled 1 and 2 on Fig. 8), whilst the single-thread channel sites did not conform with the relationship of Eaton et al. (2010) except when the dimensionless relative bank strength was set to relatively high values of ~4. For the upstream Bintacan and Abuan samples where the channel was still confined and exposed bedrock was present, these relative bank strength values are more

reasonable. Even when varying the bankfull discharge estimates by ±50% (the parameter with the most uncertainty), a number of the samples are still not consistent with the threshold proposed from the the global dataset in Mueller and Pitlick (2014). By varying channel slope by ±80% of the values derived from the IfSAR DEM, the errors bars indicate there is some overlap with the Mueller and Pitlick (2014) dataset and braided to single-thread threshold.

3.3. Channel width

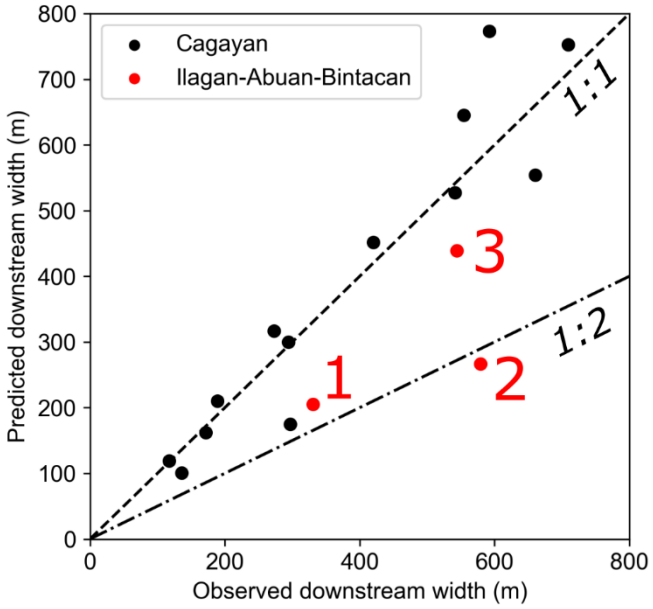

Fig. 9. Predicted and observed variations in channel width downstream of tributary junctions across the Cagayan catchment. The three red points relate to tributary junctions within the study area; 1) Upper Ilagan (near grain size site C1 on Fig. 1), 2) Bintacan-Ilagan (near grain size site C3), 3) Cagayan-Ilagan (near grain size site C4). The black dashed lines represent 1:1 and 1:2 relationships between observed and predicted channel width.

The Cagayan channel width data show a strong positive relationship between predicted and observed channel width (Fig. 9), suggesting that width scales proportionally with discharge and favours the use of b = 0.5 which was initially derived from observations in temperate systems (Leopold and Maddock, 1953; Ferguson and Hoey, 2008). Values which deviate from

433 this trend represent values where the observed channel width is generally greater than the
434 predicted value, as is evident in the three tributary junctions associated with the Cagayan-
435 Ilagan-Bintacan region (shown in red).
436
437 3.4. Sediment grain size
438
439 Sediment sizes in the main Ilagan channel are typically finer than those in either the Abuan or
440 Bintacan tributaries (Fig. 10). Grain sizes in the Abuan and Bintacan are more variable, both
441 within each sample where the sorting $(D_{84}/D_{16})^{0.5}$ is poorer, and spatially across the sampled
442 bars than in the main Ilagan channel. This variability and poor sorting are consistent with field
443 observations of coarser lateral inputs of sediment directly from adjacent hillslopes into these
444 channels, and also that tributaries to these rivers are steep and laterally confined within the
445 Sierra Madre mountains. In contrast, the Ilagan channel flows largely through a lower gradient
446 and unconfined alluvial plain. The grain sizes measured furthest downstream on the Abuan
447 and Bintacan channels (D_{84} = 75.6 and 74.1 mm, respectively) are comparable to that of the
448 Ilagan channel (D_{84} = 81.2 and 80.1 mm for sites Ilagan 2 and 3, respectively).
449
450
451
452
453
454
455
456
457

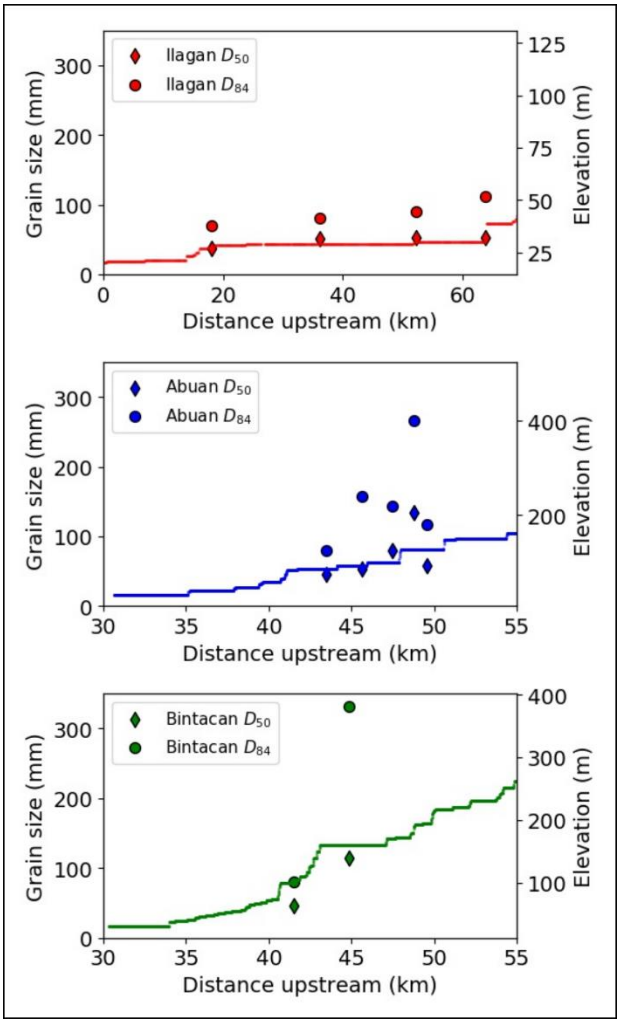

458

459 Fig. 10. D_{50} and D_{84} grain size statistics from surface grain size measurements on the Ilagan, Abuan
460 and Bintacan channels (locations shown in Fig. 1b). Long channel profiles are also shown for each
461 system, where the distance upstream is relative to the most downstream location of the study area (on
462 the Ilagan channel).

463

464 **4. Discussion**

465

466 4.1. Impact of catchment disturbance on sediment supply and transport in the Cagayan
467 catchment

468

469 Between 1987 and 2010, from analysis of satellite imagery, approximately 14% of the Isabella
470 province is suggested to have undergone deforestation (Forest Management Bureau, 2013).

Forest clearance for agricultural land on the lower gradient Ilagan floodplain is likely to have caused a reduction in bank shear strength and cohesion; this reduction may have resulted in increased rates of lateral channel migration in this part of the catchment. Changes in forest cover are less well documented in the headwaters of the Ilagan catchment where access is limited but illegal logging is reported (van der Ploeg et al., 2011), suggesting that this process may also be important further upstream but more difficult to quantify. Sediment generated and transported by typhoon storms and their associated discharges in the Bintacan and Abuan catchments, however, were observed in thick (>5 m) sedimentary deposits which persist along channel margins within the Sierra Madre mountains. Sediment generated by the mass-wasting of hillslopes, triggered by typhoon storm events, appears to be the dominant mechanism through which sediment is supplied to these rivers, rather than changes in forest cover. This is consistent with findings from other tropical systems such as the LiWu River (Taiwan) where cyclone-induced floods are thought to drive 77-92% of non-fossil particulate organic carbon erosion and transport through the catchment (Hilton et al., 2008). When considered alongside an absence of systematic change in lateral migration rates across the region over the last ~40 years (Fig. 6), there is no evidence that increased deforestation (over the same time period) in the Pinacanauan de Ilagan catchment has had any significant impact on channel morphodynamics.

4.2. Sediment dynamics in the Pinacanauan de Ilagan catchment

On exiting the mountains, the Ilagan, Abuan and Bintacan all cross lower gradient alluvial plains where in many instances coarse boulders can be observed on the surface of much finer gravel bars. Large boulders (intermediate axes >1 m in some instances) observed on the Bintacan close to site B2 were attributed to the most recent Typhoon Lawin (2016), which generated sufficient discharge to transport boulders of this size several kilometres downstream onto the alluvial plain. However, the D_{50} and D_{84} grain size measurements at sites B2 and A5 were comparable to sites upstream and downstream of their confluences with the

Ilagan River (sites C2 and C3, respectively). This suggests that coarsest sediment generated in the Sierra Madre mountains is largely contained either within the confined bedrock channels or on the part of the alluvial plain that is immediately downstream of the exit from the mountains.

Increased braiding intensity immediately downstream of the Abuan and Bintacan confluences with the Ilagan is consistent with increased sediment supply to the Ilagan from these tributaries. Finer sediment generated by typhoon-induced hillslope failure, or by reworking of existing sedimentary deposits under high discharge conditions, is likely transported from the Sierra Madre mountains by the Bintacan and Abuan channels and deposited on entering the larger Ilagan channel. This is consistent with the abrupt reduction in channel gradient between the tributaries and main Ilagan channel (Fig. 10), which would result in the rapid deposition of sediment which is too coarse to be entrained in the Ilagan channel.

4.3. The role of topographic constraints and channel aggradation on channel pattern, width, and migration

Sediment deposition or aggradation in the confluence region is likely to be enhanced by local topographic constriction of the channel immediately upstream and downstream of the tributary confluences (Fig. 11). Following the methodology of Clubb et al. (2017), swath profiling of the Ilagan-Abuan-Bintacan area using 1 m resolution LiDAR data highlights patterns of topographic relief and channel migration in the region, where landscape elevation is normalised to the elevation of the closest point on the river channel (Hergarten et al., 2014; Dingle et al., 2016; Clubb et al., 2017). Broad alluvial plains with numerous scroll bars and meander scarps can be seen immediately upstream of each zone of channel constriction, suggesting that rates of channel migration and reworking are substantially enhanced in these regions. Relatively high channel sinuosities and reduced braiding intensity on the Ilagan upstream of the Abuan confluence may be a response of the Ilagan channel to enhanced bed aggradation (caused by the topographic constrictions) and a subsequent narrowing of the

channel, forcing the channel to incise into these deposits. Interestingly, a similar pattern is observed further downstream on the Cagayan River (Fig. 7b) where channel sinuosity is considerably higher in regions immediately upstream of topographic constrictions. The prevalence of meander scarps and chute cutoffs across these regions also supports high rates of lateral channel migration. In the reach between the two lateral constrictions identified on Fig. 10, the high sediment inputs from the Bintacan and Abuan tributaries prevent the channel from incising into the alluvial floodplain. Instead the braiding intensity and rates of confluence and channel migration are elevated, resulting in more rapid recycling and reworking of the alluvial floodplain, where vertical incision is inhibited by higher rates of aggradation on the channel bed. Along the Cagayan and Ilagan Rivers, valley confinement is closely related to channel pattern and lateral channel migration rate. Regions upstream of these topographic constrictions typically have more sinuous channel planforms and undergo higher rates of lateral channel migration as a result of locally increased aggradation (due to high sediment supply). Channels incise into the alluvial plain in order to reduce their gradient, and once developed, migrate laterally in order to maintain channel capacity as sediment is transported and deposited within the reach. Where rates of bed aggradation are very high, the channel may not be able to incise vertically and, instead, braiding intensity remains high and the channel belt (and floodplain) is rapidly reworked by a series of smaller braids or channels. In contrast, as single-thread channels pass through confined regions they are more laterally stable as lateral adjustment is inhibited by high relative bank strength. The sinuosity of these confined reaches is more likely to be a function of the valley topography than flow or sediment dynamics.

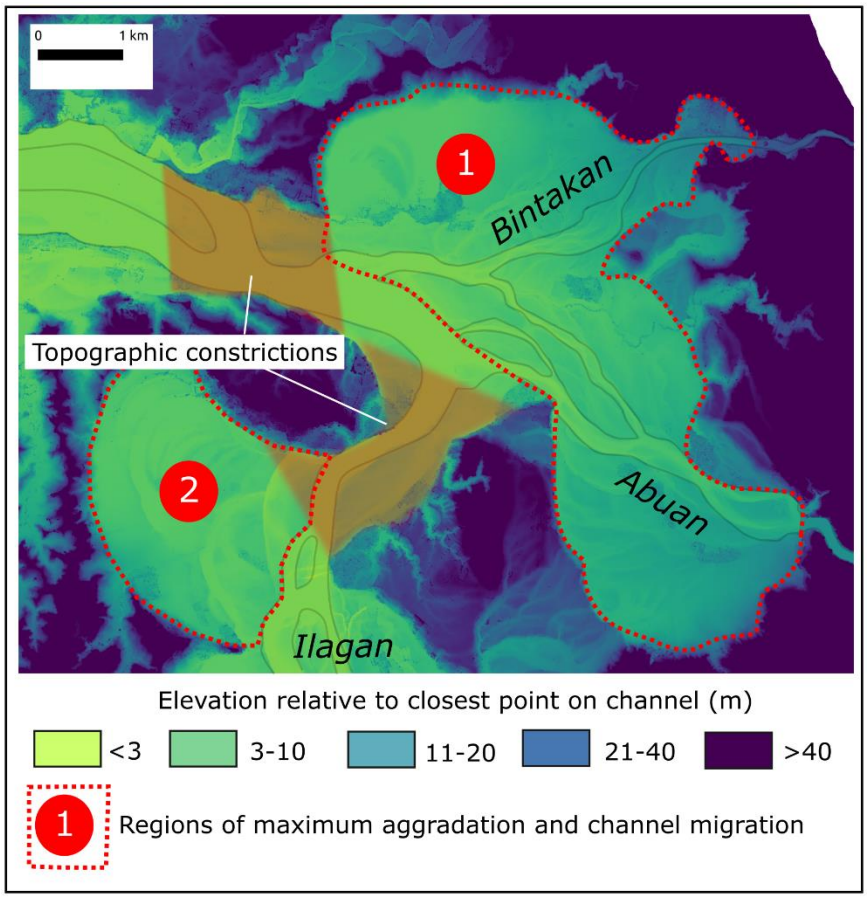

Fig. 11. Swath profile of the Ilagan-Abuan-Bintacan confluence region, highlighting the local distribution of topographic relief and lateral channel and floodplain constrictions. Elevation (shown by colours) is normalised to the elevation of the closest point on the channel. Two zones delineated by red dashed lines highlight parts of the floodplain upstream of lateral constrictions where numerous scroll bars and meander scarps are evident, suggesting regions of enhanced lateral channel migration.

Comparing new meander migration rates from this study with existing rates in a number of temperate and tropical rivers (both disturbed and undisturbed), the highest migration rates are typically observed in larger catchments (Fig. 12). These rates are independent of channel width and radius of meander curvature, which have been commonly used to non-dimensionalise migration rates for channel and catchment size (e.g., Hickin and Nanson, 1975; Hudson and Kesel, 2000; Hooke, 2007). In general, migration rates in tropical catchments for a given catchment area exceed those in temperate regions. One temperate system with large migration rates is the Lower Mississippi River (Hudson and Kesel, 2000) where meander

565 migration rates of up to 123 m/yr were observed pre-disturbance. However, although high
566 these rates are consistent with the relationship between catchment area and migration rate
567 (Fig. 12). The spatial variability in migration rates reported by Hudson and Kesel (2000) were
568 attributed to heterogeneity of floodplain deposits, where resistant clay plugs reduced migration
569 rates by forcing meander bends in these regions to develop more arcuate morphology.
570 However, the influence of variability in floodplain composition/channel bank strength (e.g., clay
571 versus poorly consolidated sand) was not considered in terms of wider channel morphology
572 and sediment transport dynamics, which may drive differences in aggradation and lateral
573 migration rates.
574
575
576
577
578
579
580
581
582
583
584
585
586
587
588
589

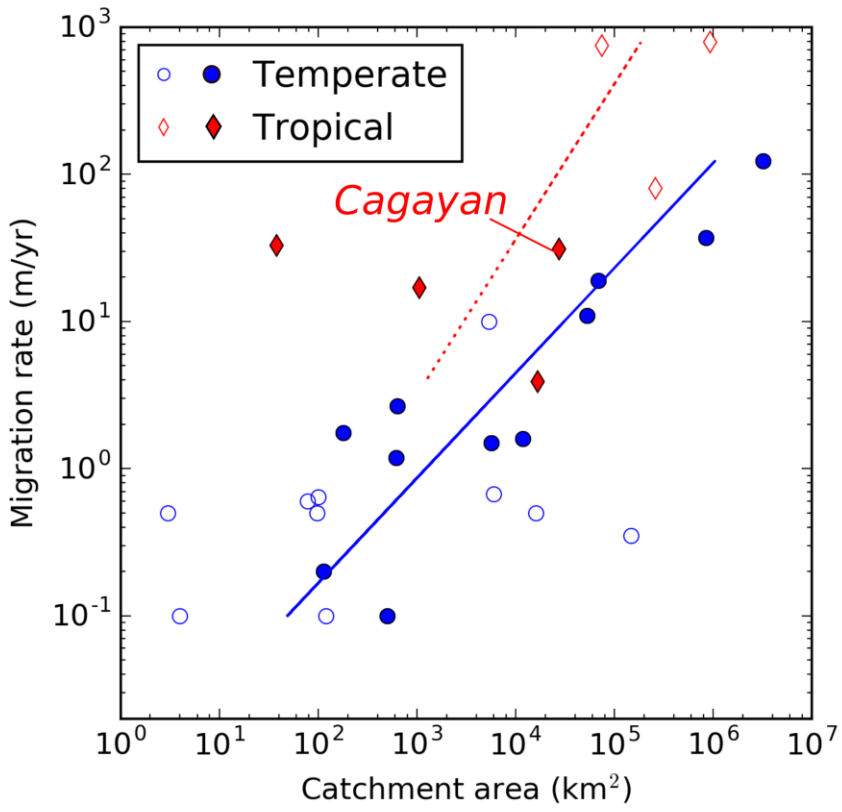

590 Fig. 12. Annual channel and meander migration rates from this and published studies (Wolman and
591 Leopold, 1957; Hooke, 1980; Lawler, 1993; Hudson and Kesel, 2000; Micheli et al., 2004; Horton et al.,
592 2017; Suizu and Nanson, 2018). Red diamonds represent data from tropical river systems, while blue
593 circles represent temperate river systems. It should be noted that these migration rates include a

combination of reach average and maximum meander migration rates, averaged over variable time periods. Where information was available, closed symbols represent maximum reported migration rates while open symbols represent a combination of mean migration rate or sources where it was not specified. Best-fit power relationships are also shown for both datasets (blue and red lines).

High aggradation rates in the Cagayan may also explain the disagreement between channel pattern, dimensionless discharge and channel gradient (Fig. 8) in comparison to global channel pattern data sets (e.g., Eaton et al., 2010; Mueller and Pitlick, 2014). Data from the single-thread Bintacan, Abuan and Ilagan channels suggest that very high relative bank strengths would be required to align with published relationships. Such high relative bank strength values are possible where the channel was laterally constrained by bedrock channel walls or very localised clay deposits within the channel bank. This suggests that using relationships such as Mueller and Pitlick's (2014) to predict channel pattern may not be fully appropriate in systems which transition between bedrock and alluvial settings where the channel is not always free to adjust its width, in systems responding transiently to changes in sediment supply, or where relative bank strength is highly variable (heterogeneous floodplain compositions). The presence of locally braided reaches suggests that many of these channels may be close to a threshold between single-thread and braided forms. The two data points on the Ilagan channel (labelled 3 on Fig. 8) based on measurements at sites C2 and C3, are also located around the Abuan and Bintacan channel confluences where aggradation rates may be periodically enhanced by high sediment inputs from these tributaries. As such, these sites may represent transient and non-regime responses to these aggradational conditions (Eaton et al., 2010). The relatively high recurrence interval of extreme sediment generating events in these headwater catchments, combined with spatial patterns of channel and valley confinement, are likely the dominant controlling factors on channel morphodynamics in the Cagayan valley.

Very few gravel-sized (or coarser) sediments were observed downstream of the Cagayan-Ilagan confluence. Grain size measurements made at location C4 were restricted to small patches of gravel exposed on the upstream end of a large sand bar. At the most downstream site on the Ilagan channel (C3), the channel is still dominated by gravel and larger sized sediments (Fig. 10). The simplest interpretation of this is that any coarse sediment delivered from the Ilagan into the Cagayan channel is rapidly buried by the comparatively larger sand flux transported by the Cagayan. Sand-bed conditions in the Cagayan may locally enhance transport of coarser sediment from the Ilagan tributary as a result of decreased bed roughness, allowing smaller patches of gravel (and coarser) sized sediments to persist in predominantly sand-bed channel conditions (Paola and Seal, 1995; Venditti and Church, 2014)

4.4. Impact of observed morphodynamics for understanding tropical river geomorphology

Tributaries draining the Sierra Madre mountains generate and transport large sediment fluxes as a result of typhoon-induced hillslope mass wasting, which are likely to be enhanced by climatically-controlled chemical and biological processes (Syvitski et al., 2014). These processes include chemical weathering of bedrock and sediments, which may accelerate the breakdown or failure of hillslopes where rock strength (or fracture density) is weakened (or increased) by chemical processes such as dissolution. Similarly, high vegetation density in tributary headwaters may further accelerate chemical and physical weathering rates via processes such as tree throw and root pry (Gabet and Mudd, 2010) which both mechanically break down and remove rock and sediment, but also expose underlying bedrock to the atmosphere. Each year several high magnitude discharge events transport these large quantities of sediment efficiently through the Ilagan and wider Cagayan catchments. When combined with low gradient channels and poorly consolidated floodplain and bank sediments in the Cagayan Valley, these flood events and high sediment discharges appear to drive accelerated rates of lateral channel and confluence migration. In turn, this results in large

quantities of the Ilagan and Cagayan floodplain sediment being recycled back into the modern channels.

While the grain size of sediment observed in the Abuan and Bintacan tributaries was relatively coarse, the majority of this sediment does not appear to be exported downstream into the Ilagan or Cagayan channels. Any deposition of sediment delivered by the Abuan and Bintacan tributaries into the Ilagan is likely to enhance local rates of lateral erosion and floodplain reworking, as a result of reduced channel capacity, which would further accelerate the burial of coarser sediments. The high sediment loads delivered from these tributaries into the Ilagan and Cagayan may also explain the observed channel widening downstream of confluences in the study area (in comparison to other parts of the Cagayan catchment and data from temperate settings), where high aggradation rates immediately downstream of these confluences locally enhance lateral erosion and channel widening.

Increased lateral channel instability associated with the Abuan, Bintacan and Ilagan confluences initiates higher rates of sediment exchange between the entire modern Cagayan channel and floodplain further downstream. Where the channel is unconfined, the banks of the Cagayan River as it passes through the Cagayan valley are typically ~10-20 m thick, poorly consolidated sand and silt deposits which are unstable even under low to moderate flow conditions. Field observations confirm that many of these banks are severely undercut, commonly in the submerged portion of the bank (even under low flow conditions). Consequently, relatively low discharges may be capable of preconditioning or even driving bank collapse and erosion along the Cagayan River (Dunne and Jerolmack, 2018).

In actively migrating reaches, the exchange of floodplain-channel material is likely to be high enough that a large portion of the sediment load exported will have spent some time stored in the floodplain (Lauer and Parker, 2008). Patterns of channel migration and channel morphology are key in determining the timescales over which sediment resides within the

676 alluvial floodplain. In theory, periods of increased sediment supply (such as those driven by
677 typhoon storms) will result in enhanced channel bed aggradation (and overbank
678 sedimentation) upstream of topographically constrained reaches of the Ilagan catchment,
679 driving an acceleration in channel reworking and lateral migration. The ability of the system to
680 transfer this sediment, generated either directly by the event or by recycling of the alluvial
681 floodplain, will be closely correlated to peak water discharges in subsequent months. In
682 tropical river systems such as the Cagayan which experience numerous typhoons each year,
683 high magnitude flow events occur frequently enough (Fig. 3) to efficiently both transport
684 sediment downstream in either suspension or as bedload, and also laterally erode into alluvial
685 banks so limiting excessive vertical aggradation of the channel bed. In regions where locally
686 braided reaches exist and the channel is close to the threshold between braided and single-
687 thread, these large sediment generating events may cause (temporary) changes in channel
688 pattern until the channel is able to mobilise these deposits.
689
690 It is not possible at present to directly test whether sediment generated by high rates of
691 floodplain recycling represents a significant proportion of the total sediment flux of the entire
692 Cagayan catchment, as direct and reliable sediment concentration or flux measurements are
693 not openly available. Data discussed in Principe (2012), based on monthly sediment yield data
694 between 2002-2007 at Bangag monitoring station (close to the Cagayan outlet) were used to
695 calibrate a SWAT (Soil and Water Assessment Tool) model of the Cagayan catchment which
696 produced a simulated average sediment yield of 115 tonnes/ha/yr based on 2012 land use
697 patterns. This sediment yield converts to an annual sediment flux of 317 Mt/yr, which is our
698 only estimate of sediment flux for the Cagayan River. The yield can also be converted to a
699 catchment-average denudation rate of 4.3-7.1 mm/yr, depending on the density of eroded
700 material. This range of values is based on the density of quartz (2650 kg/m^3) and for
701 uncompacted sand as might be expected across some of the Cagayan alluvial floodplain
702 (1600 kg/m^3) and, as such, represents the widest range of possible values. Even the lower
703 end of this range of values places the catchment-averaged denudation rate calculated here

among some of the highest rates from tectonically active mountain ranges globally (Montgomery and Brandon, 2002). Robust conclusions regarding the sediment budget of the Cagayan River are therefore difficult to make in the absence of openly available or spatially and temporally extensive sediment discharge gauging data. Syvitski et al. (2014) suggested that tropical rivers do not carry more particulate load to the oceans in comparison to more temperate systems, based on BQART modelling using average water discharge measurements. However, this modelling approach is likely to underestimate sediment flux where the annual sediment flux transport is dominated by short-lived, very high magnitude discharge events during typhoons.

4.5. Consequences for river and flood risk management

The observed dynamism of channels in the study area suggests that sediment supply and channel migration are likely to change channel capacity and flow routing, and thus the associated flood and erosion risk to people, property and infrastructure. The area investigated here was chosen to be representative of catchments across the Philippines with similar characteristics. Our results imply that geomorphological change impacts flood risk, and that specific examples of this can be identified (Fig. 4). Our results show the significance of both aggradation and erosion, each of which has been identified as frequently being overlooked in flood risk management (Lane et al. 2007; Slater, 2016). Flood risk mapping in the Philippines has largely been undertaken as part of the Nationwide Operational Assessment of Hazards project (Lagmay et al., 2017) using two-dimensional hydraulic modelling over airborne-LiDAR derived topography. This approach has led to a step change in the understanding of flood risk but the existing modelling framework does not incorporate the impacts of topographic change on flood levels and routing. The results from this paper need to be extended to other catchments and can then be used to inform a national-scale assessment to identify river reaches that are most susceptible to geomorphic change. For susceptible reaches, a sediment budgeting approach (Frings et al., 2018) could be applied to quantify channel change using

repeat topographic surveys. These data could then be used to improve flood risk modelling, including the application of morphodynamic models (Williams et al., 2016).

Responses to river bank erosion by river managers range from hard engineering to prevent lateral erosion (Przedwojski et al., 2005) to the creation of erodible river corridors where rivers are given space to naturally migrate (Piégay et al., 2005; Biron et al., 2014). Within the Cagayan catchment, hard bank protection structures have been, and continue to be, constructed along eroding banks that are adjacent to vulnerable property, particularly residential areas. In temperate regions where rivers are subject to high rates of sediment supply, hard bank protection structures that narrow river corridors can cause increased aggradation (Davies et al., 2003; Siviglia et al., 2008) and thus can increase flood risk due to reduced channel capacity and greater risk of flood defence breaches. However, rivers that are confined by bank protection and subject to high rates of sediment supply may also respond by steepening and/or fining their bed to enable greater sediment transport rates (Eaton and Church, 2009; Madej et al., 2009). The complexity of these geomorphological responses to river corridor confinement and intermittent sediment supply suggests that further observational data and numerical scenario modelling is needed to enable a sustainable approach to managing river dynamism and land development within the Cagayan catchment.

5. Conclusions

Rates and patterns of channel and confluence migration, combined with channel pattern, width and sediment grain size analysis along ~85 km of the Cagayan River and a number of its tributaries suggest that sediment transport and deposition are key components of tropical river morphodynamics. In these fluvial systems, sediment loads are typically high and annual flow hydrographs are dominated by typhoon storms which generate several geomorphically effective flows each year. Typhoon related discharges mobilise and recycle large quantities of hillslope and floodplain sediment, which has a direct impact on channel morphology (channel

760 sinuosity, width, braiding intensity) and lateral channel and confluence migration rates. There
761 is no clear evidence that land use change within the Cagayan catchment has led to an increase
762 in lateral channel migration rates over the last ~40 years. In the case of the Cagayan River,
763 spatial variations in floodplain width and heterogeneity may also enhance local rates of bed
764 aggradation and channel mobility, most notably around major channel confluences where
765 tributaries have larger or coarser sediment loads. An analysis of existing migration rate data
766 in combination with new rates from the Cagayan River also suggest that channel migration
767 rates are typically greater in tropical rivers than in temperate systems. Regions of increased
768 bed aggradation at confluences and upstream of topographic valley constrictions may also
769 explain why published relationships between slope and dimensionless discharge for
770 discriminating braided and single-thread channels may not be fully appropriate for aggrading
771 tropical river systems. We propose that these factors need to be taken into consideration in
772 wider river and flood management programmes in these types of settings where flood risk
773 mapping may need to incorporate channel dynamism and hard bank protection may result in
774 geomorphological feedbacks that have adverse consequences for flood risk.
775
776 Acknowledgements
777
778 This research was funded by the Scottish Funding Council, grant number SFC-AN-12-2017.
779 We thank the City Government of Ilagan for supporting fieldwork access and logistics. Meghan
780 Oliver provided the data for Fig. 9. We also thank Avijit Gupta and an anonymous reviewer for
781 comments and discussions that have helped to improve this paper.
782
783 Data availability
784
785 Satellite data used in the migration analysis was freely downloaded from the USGS Earth
786 Explorer website (http://earthexplorer.usgs.gov/). IfSAR data were generated by Intermap Inc.
787 for the National Mapping and Resource Information Autority (NAMRIA) between January and

July 2013. Digitised channel banks and centrelines are provided as ESRI Shapefiles in the online Supplementary Material, in addition to sinuosity and braiding data and sediment grain size statistics. The swath profiling tool from Clubb et al. (2017) is freely available to download from http://github.com/LSDtopotools/LSDTopoTools_FloodplainTerraceExtraction. Hydrological data were provided by the Bureau of Research Standards under the Philippines Department of Public Works and Highways. The dataset generated for this manuscript is available from the Mendeley data repository: DOI:10.17632/sn9mzzpxtn.2.

References

Aalto, R., Lauer, J.W., Dietrich, W.E., 2008. Spatial and temporal dynamics of sediment accumulation and exchange along Strickland River floodplains (Papua New Guinea) over decadal-to-centennial timescales. Journal of Geophysical Research: Earth Surface 113 (F01S04).

Alfieri, L., Bisselink, B., Dottori, F., Naumann, G., de Roo, A., Salamon, P., Wyser, K., Feyen, L., 2017. Global projections of river flood risk in a warmer world. Earth's Future 5 (2), 171-182.

Ashmore, P. E., 2013. Morphology and Dynamics of Braided Rivers. In: Shroder, J. (Editor in Chief), Wohl, E. (Ed.), Treatise on Geomorphology. Academic Press, San Diego, CA, vol. 9, Fluvial Geomorphology, 289-312.

Ashworth, P.J., Lewin, J., 2012. How do big rivers come to be different? Earth-Science Reviews, 114 (1-2), pp.84-107.

Balderama, O. F. Alejo, L. A., Tongson, E., Rhia, E., Pantola, T., 2017. Development and Application of Corn Model for Climate Change Impact Assessment and Decision Support System: Enabling Philippine Farmers Adapt to Climate Variability In: Walter Leal Filho (Eds.), Climate Change Research at Universities, 373-387.

Best, J.L., Ashworth, P.J., 1997. Scour in large braided rivers and the recognition of sequence stratigraphic boundaries. Nature 387 (6630), 275-277.

816 Biron, P. M., Buffin-Bélanger, T., Larocque, M., Choné, G., Cloutier, C. A., Ouellet, M. A.,
817 Demers, S., Olsen, T., Desjarlais, C., Eyquem, J., 2014. Freedom Space for Rivers: A
818 Sustainable Management Approach to Enhance River Resilience, Environmental
819 Management 54 (5), 1056-1073.
820 Church, M., 1992. Channel morphology and typology. The Rivers Handbook: Hydrological and
821 Ecological Principles. P. Calow and G. Petts (editors). Blackwell Scientific Publications,
822 Oxford, UK.
823 Church, M., 2006. Bed material transport and the morphology of alluvial river channels. Ann.
824 Rev. Earth Planet. Sci. 34, 325-354.
825 Clubb, F.J., Mudd, S.M., Attal, M., Milodowski, D.T., Grieve, S.W., 2016. The relationship
826 between drainage density, erosion rate, and hilltop curvature: Implications for sediment
827 transport processes. Journal of Geophysical Research: Earth Surface 121 (10), 1724-
828 1745.
829 Clubb, F.J., Mudd, S.M., Milodowski, D.T., Valters, D.A., Slater, L.J., Hurst, M.D., Limaye,
830 A.B., 2017. Geomorphometric delineation of floodplains and terraces from objectively
831 defined topographic thresholds. Earth Surface Dynamics 5 (3), 369-385.
832 Constantine, C.R., Dunne, T., Hanson, G.J., 2009. Examining the physical meaning of the
833 bank erosion coefficient used in meander migration modeling. Geomorphology 106 (3-
834 4), 242-252.
835 Constantine, J.A., Dunne, T., Ahmed, J., Legleiter, C., Lazarus, E.D., 2014. Sediment supply
836 as a driver of river meandering and floodplain evolution in the Amazon Basin. Nature
837 Geoscience 7 (12), 899-903.
838 Dade, W.B., 2000. Grain size, sediment transport and alluvial channel
839 pattern. Geomorphology 35 (1-2), 119-126.
840 Darby, S.E., Leyland, J., Kummu, M., Räsänen, T.A., Lauri, H., 2013. Decoding the drivers of
841 bank erosion on the Mekong river: The roles of the Asian monsoon, tropical storms, and
842 snowmelt. Water Resources Research 49 (4), 2146-2163.

843 Davies, T.R., McSaveney, M.J., Clarkson, P.J. 2003. Anthropic aggradation of the Waiho
844 River, Westland, New Zealand: microscale modelling. Earth Surface Processes and
845 Landforms 28 (2), 209-218.
846 Dewan, A., Corner, R., Saleem, A., Rahman, M.M., Haider, M.R., Rahman, M.M., Sarker,
847 M.H., 2017. Assessing channel changes of the Ganges-Padma River system in
848 Bangladesh using Landsat and hydrological data. Geomorphology 276, 257-279.
849 Dietrich, W.E., Smith, J.D., Dunne, T., 1979. Flow and sediment transport in a sand bedded
850 meander. The Journal of Geology 87 (3), 305-315.
851 Dingle, E.H., Sinclair, H.D., Attal, M., Milodowski, D.T., Singh, V., 2016. Subsidence control
852 on river morphology and grain size in the Ganga Plain. American Journal of Science 316
853 (8), 778-812.
854 Dixon, S.J., Smith, G.H.S., Best, J.L., Nicholas, A.P., Bull, J.M., Vardy, M.E., Sarker, M.H.,
855 Goodbred, S., 2018. The planform mobility of river channel confluences: Insights from
856 analysis of remotely sensed imagery. Earth-Science Reviews 176, 1-18.
857 Dunne, K.B., Jerolmack, D.J., 2018. Evidence of, and a proposed explanation for, bimodal
858 transport states in alluvial rivers. Earth Surface Dynamics 6 (3), 583-594.
859 Durkee, E.F., Pederson, S.L., 1961. Geology of northern Luzon, Philippines. AAPG Bulletin 45
860 (2), 137-168.
861 Eaton, B.C., Church, M., 2009. Channel stability in bed load–dominated streams with
862 nonerodible banks: Inferences from experiments in a sinuous flume. Journal of
863 Geophysical Research: Earth Surface 114 (F01024).
864 Eaton, B.C., Millar, R.G., Davidson, S., 2010. Channel patterns: Braided, anabranching, and
865 single-thread. Geomorphology 120 (3-4), 353-364.
866 Ferguson, R.I., Cudden, J.R., Hoey, T.B., Rice, S.P., 2006. River system discontinuities due
867 to lateral inputs: generic styles and controls. Earth Surface Processes and Landforms
868 31, 1149–1166.
869 Ferguson, R., Hoey, T., 2008. Effects of tributaries on main-channel geomorphology. River
870 confluences, tributaries and the fluvial network, 183-208.

871 Floresca, J.P., Paringit, E. C., 2017. Overview of the Program and the Pinacanauan de Ilagan
872 River. In Paringit, E.C. (Ed.), LIDAR Surveys and Flood Hazard Mapping of the
873 Philippines, University of the Philippines Training Center for Applied Geodesy and
874 Photogrammetry, Quezon City, 371.
875 Forest Management Bureau, 2013. Philippine Forest Facts and Figures. Department of
876 Environment and Natural Resources, Philippines. Second Edition.
877 [http://forestry.denr.gov.ph/pdf/ref/PF3_2013.pdf; accessed online 04/09/2018]
878 Frings, R. M., Ten Brinke, W. B. M., 2018. Ten reasons to set up sediment budgets for river
879 management, International Journal of River Basin Management 16 (1), 35-40.
880 Gabet, E.J., Mudd, S.M., 2010. Bedrock erosion by root fracture and tree throw: A coupled
881 biogeomorphic model to explore the humped soil production function and the
882 persistence of hillslope soils. Journal of Geophysical Research: Earth Surface 115 (F4).
883 Gran, K.B., Montgomery, D.R., Halbur, J.C., 2011. Long-term elevated post-eruption
884 sedimentation at Mount Pinatubo, Philippines. Geology 39 (4), 367-370.
885 Hergarten, S., Robl, J., Stüwe, K., 2014. Extracting topographic swath profiles across curved
886 geomorphic features. Earth Surface Dynamics 2 (1), 97-104.
887 Hickin, E.J., Nanson, G.C., 1975. The character of channel migration on the Beatton River,
888 northeast British Columbia, Canada. Geological Society of America Bulletin 86 (4), 487-
889 494.
890 Hilton, R.G., Galy, A., Hovius, N., Chen, M.C., Horng, M.J., Chen, H., 2008. Tropical-cyclone-
891 driven erosion of the terrestrial biosphere from mountains. Nature Geoscience 1 (11),
892 759-762.
893 Hooke, J.M., 2007. Spatial variability, mechanisms and propagation of change in an active
894 meandering river. Geomorphology 84 (3-4), 277-296.
895 Hooke, J.M., 1980. Magnitude and distribution of rates of river bank erosion. Earth Surface
896 Processes 5 (2), 143-157.

Horton, A.J., Constantine, J.A., Hales, T.C., Goossens, B., Bruford, M.W., Lazarus, E.D., 2017. Modification of river meandering by tropical deforestation. Geology 45 (6), 511-514.

Hudson, P.F., Kesel, R.H., 2000. Channel migration and meander-bend curvature in the lower Mississippi River prior to major human modification. Geology 28 (6), 531-534.

Lagmay, A. M. F., Racoma, B.A., Aracan, K.A., Alconis-Ayco, J., Saddi, I.L., 2017. Disseminating near-real-time hazards information and flood maps in the Philippines through Web-GIS, Journal of Environmental Sciences 59, 13-23.

Lane, S. N., Tayefi, V., Reid, S.C., Yu, D., Hardy, R.J., 2007. Interactions between sediment delivery, channel change, climate change and flood risk in a temperate upland environment, Earth Surface Processes and Landforms 32 (3), 429-446.

Latrubesse, E.M., Stevaux, J.C., Sinha, R., 2005. Tropical rivers. Geomorphology 70 (3), 187-206.

Lauer, J.W., Parker, G., 2008. Net local removal of floodplain sediment by river meander migration. Geomorphology 96 (1-2), 123-149.

Lawler, D.M., 1993. The measurement of river bank erosion and lateral channel change: a review. Earth Surface Processes and Landforms 18 (9), 777-821.

Leopold, L.B., Maddock, T., 1953. The hydraulic geometry of stream channels and some physiographic implications (Vol. 252). US Government Printing Office.

Leopold, L.B., Wolman, M.G., 1957. River channel patterns: braided, meandering, and straight. US Geological Survey Professional Paper 282-B, 85.

Madej M.A., Sutherland D.G., Lisle T.E., Pryor, B. 2009. Channel responses to varying sediment input: A flume experiment modeled after Redwood Creek, California. Geomorphology 103, 507–519.

McMillan, H., Freer, J., Pappenberger, F., Krueger, T., Clark, M., 2010. Impacts of uncertain river flow data on rainfall- runoff model calibration and discharge predictions. Hydrological Processes 24 (10), 1270-1284.

924 Micheli, E.R., Kirchner, J.W., Larsen, E.W., 2004. Quantifying the effect of riparian forest
925 versus agricultural vegetation on river meander migration rates, Central Sacramento
926 River, California, USA. River Research and Applications 20 (5), 537-548.
927 Milliman, J.D., Meade, R.H., 1983. World-wide delivery of river sediment to the oceans. The
928 Journal of Geology 91 (1), 1-21.
929 Miller, D.J., Benda, L.E., 2000. Effects of punctuated sediment supply on valley-floor
930 landforms and sediment transport. Geological Society of America Bulletin 112 (12),
931 1814-1824.
932 Mines and Geosciences Bureau. 2010. Geology of the Philippines, Second Edition. Pp. 115-
933 116, 120-121.
934 Montgomery, D.R., Brandon, M.T., 2002. Topographic controls on erosion rates in tectonically
935 active mountain ranges. Earth and Planetary Science Letters 201 (3-4), 481-489.
936 Mosley, M.P., 1981. Semi-determinate hydraulic geometry of river channels, South Island,
937 New Zealand. Earth Surface Processes and Landforms 6 (2), 127-137.
938 Mueller, E.R., Pitlick, J., 2014. Sediment supply and channel morphology in mountain river
939 systems: 2. Single thread to braided transitions. Journal of Geophysical Research: Earth
940 Surface 119 (7), 1516-1541.
941 Parker G., 1979. Hydraulic geometry of active gravel rivers. Journal of the Hydraulics Division
942 ASCE 105, 1185–1201.
943 Perron, J.T., Dietrich, W.E., Kirchner, J.W., 2008. Controls on the spacing of first-order
944 valleys. Journal of Geophysical Research: Earth Surface 113 (F04016).
945 Piégay, H., Darby, S.E., Mosselman, E., Surian, N., 2005. A review of techniques available for
946 delimiting the erodible river corridor: a sustainable approach to managing bank erosion,
947 River Research and Applications 21 (7), 773-789.
948 Plink-Björklund, P., 2015. Morphodynamics of rivers strongly affected by monsoon
949 precipitation: review of depositional style and forcing factors, Sedimentary Geology 323,
950 110-147.

951 Principe, J.A., 2012. Exploring climate change effects on watershed sediment yield and land
952 cover-based mitigation measures using swat model, RS and GIS: case of Cagayan
953 River Basin, Philippines. Int. Arch. Photogram. Rem. Sens. Spatial Inform. Sci. 39, 193-
954 198.
955 Przedwojski, B., Błażejewski, R., Pilarczyk, K. W. 1995. River training techniques:
956 fundamentals, design and applications. AA Balkema, Rotterdam, 625.
957 Rice, S., Church, M., 1996. Sampling surficial fluvial gravels: The precision of size distribution
958 percentile estimates. Journal of Sedimentary Research 66, 654-65.
959 Richards, K.S., 1980. A note on changes in channel geometry at tributary junctions. Water
960 Resources Research 16 (1), 241-244.
961 Rojas, D.S., 2014. Abuan Integrated Watershed Program: Flood Hydrology and Hydraulics.
962 WWF-Philippines.
963 Samuels, P.G., 1989. Backwater lengths in rivers. Proceedings of the Institution of Civil
964 Engineers 87 (4), 571-582.
965 Scatena, F.N., Gupta, A., 2013. Streams of the montane humid tropics. In: Shroder, J. (Editor
966 in Chief), Wohl, E. (Ed.), Treatise on Geomorphology. Academic Press, San Diego, CA,
967 vol. 9, Fluvial Geomorphology, 595–611.
968 Schumm, S.A., 1985. Patterns of alluvial rivers. Annual Review of Earth and Planetary
969 Sciences 13 (1), 5-27.
970 Siviglia A., Repetto R., Zolezzi G., Tubino, M., 2008. River bed evolution due to channel
971 expansion: general behaviour and application to a case study (Kugart River, Kyrgyz
972 Republic). River Research and Applications 24, 1271–1287.
973 Slater, L. J., 2016. To what extent have changes in channel capacity contributed to flood
974 hazard trends in England and Wales?, Earth Surface Processes and Landforms 41 (8),
975 1115-1128.
976 Smith, N.D., Smith, D.G., 1984. William River: An outstanding example of channel widening
977 and braiding caused by bed-load addition. Geology 12, 78–82.

978 Suizu, T.M., Nanson, G.C., 2018. Temporal and spatial adjustments of channel migration and
979 planform geometry: responses to ENSO driven climate anomalies on the tropical freely-
980 meandering Aguapeí River, São Paulo, Brazil. Earth Surface Processes and Landforms
981 43, 1636-1647.
982 Syvitski, J.P., Cohen, S., Kettner, A.J., Brakenridge, G.R., 2014. How important and different
983 are tropical rivers? An overview. Geomorphology 227, 5-17.
984 Tolentino, P.L.M., Poortinga, A., Kanamaru, H., Keesstra, S., Maroulis, J., David, C.P.C.,
985 Ritsema, C.J., 2016. Projected impact of climate change on hydrological regimes in the
986 Philippines. PloS one 11 (10), 1-14.
987 Tucker, G.E., Slingerland, R., 1997. Drainage basin responses to climate change. Water
988 Resources Research 33 (8), 2031-2047.
989 Van den Berg, J.H., 1995. Prediction of alluvial channel pattern of perennial
990 rivers. Geomorphology 12 (4), 259-279.
991 Van der Ploeg, J., Van Weerd, M., Masipiqueña, A.B., Persoon, G.A., 2011. Illegal logging in
992 the Northern Sierra Madre Natural Park, the Philippines. Conservation and Society 9 (3),
993 202-215.
994 Williams, R.D., Measures, R., Hicks, D.M., Brasington, J., 2016. Assessment of a numerical
995 model to reproduce event-scale erosion and deposition distributions in a braided
996 river. Water Resources Research 52 (8), 6621-6642.
997 Wobus, C.W., Tucker, G.E., Anderson, R.S., 2006. Self-formed bedrock
998 channels. Geophysical Research Letters 33 (18).
999 Wolman, M.G., 1954. A method of sampling coarse river-bed material. EOS, Transactions
1000 American Geophysical Union 35 (6), 951-956.
1001 Wolman, M.G., Leopold, L.B., 1957. River flood plains: some observations on their
1002 formation (No. 282-C). US Government Printing Office, 87-109.
1003
1004
1005

Supplementary Material

Table S1. Satellite imagery sources and horizontal spatial resolution used in this study.

Year (Month)	Dataset	Horizontal spatial resolution (m)
1973 (June)	Landsat 1 MSS	60
1990 (Feb)	Thematic Mapper 1984-1997	30-50
2001 (June)	ETM+ Pan sharpened mosaic	14.25
2008 (June)	Landsat 5 TM	30
2017 (April/Nov)	Sentinel 2	10-20 (depending on band combination used)
2017 (July)	RapidEye	5